DOI: https://doi.org/10.24297/jap.v23i.9732

Precise Determination of Quantum Size Effect, Reactivity Size and Energy Levels of CdSe Nanoparticles Using Egypt Pyramids Model for Nanotechnology

Tarek El Ashram

Physics Department, College of Science, Port Said University, Port Said, Egypt

E-mails: tnelashram@sci.psu.edu.eg, tnelashram@gmail.com

Abstract

Nowadays, nanotechnology produces a variety of materials and devices, which are important for different applications. However, without a predictive successful model, it takes much more effort, money, and time to get the desired structure suitable for a certain application. Therefore, we aim to apply a new model called Egypt Pyramids Model for Nanotechnology (EPMN) on the two structures of the semiconductor compound CdSe to explain its electronic structures and properties of bulk and nanostructures. Here we show that by applying EPMN on CdSe, the quantum size effect QSE and reactivity size RS were calculated to be 5.45, 2.42, 12.61, 5.6 nm for cubic and hexagonal CdSe, respectively. The observed peaks in absorption and photoluminescence spectra, 678, 529, 457, and 325 nm, match very well the calculated transitions 626.18, 527.59, 455.82, and 326.27 nm, respectively.

Keywords: Egypt Pyramids Model, Nanotechnology, Tarek's law, Energy levels, CdSe.

1. Introduction

1.1 Nanotechnology

Nowadays nanotechnology produces a variety of materials and devices, which are important for different applications [1-10]. Yekimov attributed the new properties of nanomaterials to the quantum size effect (**QSE**) [11-15]. It is thought that the energy is continuous in both valence band and conduction band of the bulk material and by decreasing size of the particle its energy levels become discrete. Moreover, the energy gap increases by decreasing the particle size [16-20]. Actually, the energy levels are discrete in the bulk and nanostructures as explained by the crystalline accommodation law quantum quantitative model CALQQM [21-23]. CALQQM gives the exact relation between the crystal structure and the electronic energy band structure. In addition, it could explain successfully the superconductivity at room temperature, energy levels, and work functions of materials [22]. CALQQM predicted, with high accuracy, the electronic properties such as energy gaps and spectra of variety of elements in a good agreement with experimental results [23]. Tarek's law [22, 23] gives the energy levels ($\mathbf{E_N}$) of the valence band (VB) and the conduction band (CB) as the following;

$$\mathbf{E_N = T\,(NV_B)^{2/3}} \qquad (1)$$

where **T** is Tarek's constant = 1.46622 eV Å^2, $\mathbf{V_B}$ is the volume of Brillouin zone (BZ), N = 0.5, 1, 1.5, 2, 2.5,.....,F,.....,V and F is label of the Fermi level $\mathbf{E_F}$ and V is the label of the internal vacuum level $\mathbf{E_V}$.

Each **BZ** has two energy levels for two electrons of opposite spins. The most important parameter that determines the energy levels in Tarek's law is the volume of quantum state $\mathbf{V_B}$ which is given by;

$$\mathbf{V_B = 8\pi^3 / V_P} \qquad (2)$$

where $\mathbf{V_P}$ is volume of the primitive cell. The primitive cell (PC) is the smallest repetitive structural unit in the solid, which carry the chemical identity of the solid. Primitive cell has only one lattice point this lattice point may contains one atom or many atoms, the smallest primitive cell contains only one atom. In the bulk structure, if PCs are repeated periodically through the solid, this gives a single crystal structure. If a group of PCs is repeated in certain direction and the other groups are repeated in other directions, this gives polycrystalline structure. Polycrystalline materials include microcrystalline and nanocrystalline structures according to the grain size. Nanocrystalline materials have grain size ranges from 1.5 to 100 nm. The amorphous structure has a short-range order smaller than 1.5 nm. Even in the amorphous structure, PCs preserve their structures but they are randomly oriented. A nanoparticle consists of several PCs in bulk, powder, or colloidal structures. In either case, Tarek's law can determine the energy levels of any of the previous structures.

1.2 Egypt Pyramids Model for Nanotechnology (EPMN)

The band unit (BU) and space unit (SU) are new concepts in solid-state physics were introduced by CALQQM [21-23]. Each material has BU in which all electronic transitions and interactions occur. The BU is defined as the band, which contains both valence band (VB) and conduction band (CB). VB represents the filled states up to the highest energy level, which is the Fermi level ($\mathbf{E_F}$). CB represents the empty higher states up to the highest energy level, which is the internal vacuum level ($\mathbf{E_V}$). The BU of the solid can be represented as;

$$\mathbf{BU = N_F BZ + N_C BZ} \quad (3)$$

where $\mathbf{N_F}$ is the number of filled states in the VB and $\mathbf{N_C}$ is the number of empty states in the CB. For each quantum state (BZ) in energy space, there is a primitive cell (PC) in the real space. BZ is repeated in energy space as PC is repeated in real space. Therefore, for every BU in energy space, there is SU in the real space, in which the number of primitive direct cells equal to the number of states in BU. Each BZ has two energy levels for two electrons of opposite spins. The number of BUs per unit volume $\mathbf{N_{BU}}$ is given by**;**

$$\mathbf{N_{BU} = N_B / N_U} \quad (4)$$

$$\mathbf{N_U = N_F + N_C} \quad (5)$$

where $\mathbf{N_U}$ is the number of BZs in BU, and $\mathbf{N_B}$ is the number of BZs per unit volume, which is equal to the number of PCs per unit volume $\mathbf{N_P}$. SU has a certain size according to the crystal structure. If the particle size (**PS**) is smaller than the size of the SU of the bulk, the quantum size effect starts. If the size of SU is decreased further, the corresponding BU will be clipped according to the new SU size. Consequently, the properties of the material will change. We can determine the new properties from the energy levels of the new BU. The size of the space unit (**SUS**) is given by;

$$\mathbf{SUS = N_U\ PCS} \quad (6)$$

where **PCS** is the size of the primitive cell and $\mathbf{N_U}$ is the number of primitive cells in the SU. For cubic system we have one size for the three directions **PCS = a** , hence

$$\mathbf{SUS = N_U\, a} \quad \mathrm{N}\ (7)$$

where a is the lattice parameter of the cubic system. For the other crystalline systems, we have three sizes for the three directions x, y, and z.

$$\mathbf{SUS_x = N_U\, a_x\ ,\ SUS_y = N_U\, a_y\ ,\ SUS_z = N_U\, a_z} \quad (8)$$

The size with largest lattice parameter is chosen. The size of the quantum effect (**QSE**) can be defined as the size at which the BU becomes different from that of the bulk material and is given by;

$$\mathbf{PCS < RS < QSE < SUS} \quad (9)$$

where RS is the reactivity size. It is equal to the size of the valence band (**VBS**). When **PS** is decreased further until BU consists only of VB and hence $\mathbf{E_V = E_F}$. Therefore, the reactivity size can be defined as the size at which the BU consists only of VB (filled states). In this case, the particle becomes very reactive, since the electrons in the VB tend to form stable structure by interaction with the surrounding medium. The smallest VB contains only one BZ so that the smallest size of the SU is equal to the **PCS**. It is not possible to get size smaller than the size of the primitive cell even in the amorphous structure.

1.3 Cadmium Selenide Compound

Cadmium Selenide (CdSe) is a very important semiconductor compound for optoelectronic devices [24-29]. CdSe can exist in three different allotropic crystalline forms according to the temperature and pressure, wurtzite (hexagonal), zinc-blende (cubic) and rock-salt (cubic). Zinc-blende (cubic) structure is unstable and converts to the wurtzite (hexagonal) form upon heating. The transition starts at about 130 °C, and ends at 700 °C within a day. The rock-salt structure is only observed under high pressure [30, 31]. The absorption band edge of the bulk CdSe lies at 1.7 eV for both hexagonal and zinc-blende structures at room temperature [31]. Various CdSe nanostructures were obtained by [32]. Luo et al [33] have reported CdSe nano-ribbons based photodetectors with a photo response around 650 nm without using any external filter. Authors [34] observed that the introduction of CdSe QDs improved the absorption in the region of 400-560 nm. Without a predictive successful model, it takes much more efforts, money and time to get the desired structure suitable for a certain application. Therefore, the aim of the present work is to apply CALQQM and EPMN on the two structures of CdSe (hexagonal and cubic (zinc-blende)) to explain its electronic structure and properties both in bulk and nanostructures. In addition, we will verify the validity of EPMN as a predictive model for nanotechnology.

2. Computational Methodology

The computations are based on the two models CALQQM [21-23] and the present model EPMN. The lattice parameters of CdSe structures were determined from the XRD data shown in Table 1 [35]. Our first task is to find the BU of each structure of CdSe (cubic and hexagonal) and the corresponding SU using CALQQM. Secondly, we can determine each of the following parameters; $\mathbf{V_B}$, **PCS**, $\mathbf{N_U}$, **SUS**, **QSE**, and **RS** using Eqs. (1-10) of EPMN. The energy levels $\mathbf{E_N}$ were calculated using Tarek's law [22, 23] and $\mathbf{E_F}$ was calculated using crystalline accommodation law (CAL) [21].

Table 1 The lattice parameters of CdSe structures [35].

Compound	Card no.	Cry. St.	**a** (Å)	**c** (Å)
CdSe	88-2346	Cubic $F\bar{4}3m$	6.077	
CdSe	77-2307	Hex. $P6_3/mc$	4.299	7.01

3. Results and Discussion

3.1. Energy Band Structures of CdSe Bulk and Nanostructures

Fig 1 shows the energy band structure of bulk cubic CdSe compound and its variation with particle size. It is evident that as the particle size decreases, the BU is clipped without variation in energy gap and the energy levels are reduced. The bulk BU has $\mathbf{E_F}$ = 9.95 eV, $\mathbf{E_V}$ = 17.08 eV and the first level in the CB is $\mathbf{E_{C1}}$=10.76 eV. The BU consists of **VB = 4BZs** and **CB = 5BZs** so that $\mathbf{N_U}$ = 9. The size of the SU of the bulk is 5.45 nm, this is the size of quantum effect at which BU becomes different from that of the bulk structure. Thus, **QSE** for cubic CdSe is < 5.45 nm. As the particle size decreases further, more clipping occurs until we get the reactive size (**RS** = 2.42 nm) at which the BU consists only of VB in this case $\mathbf{E_V = E_F}$. The detail of the band structures of bulk cubic CdSe and their nanostructure is given in Table 2.

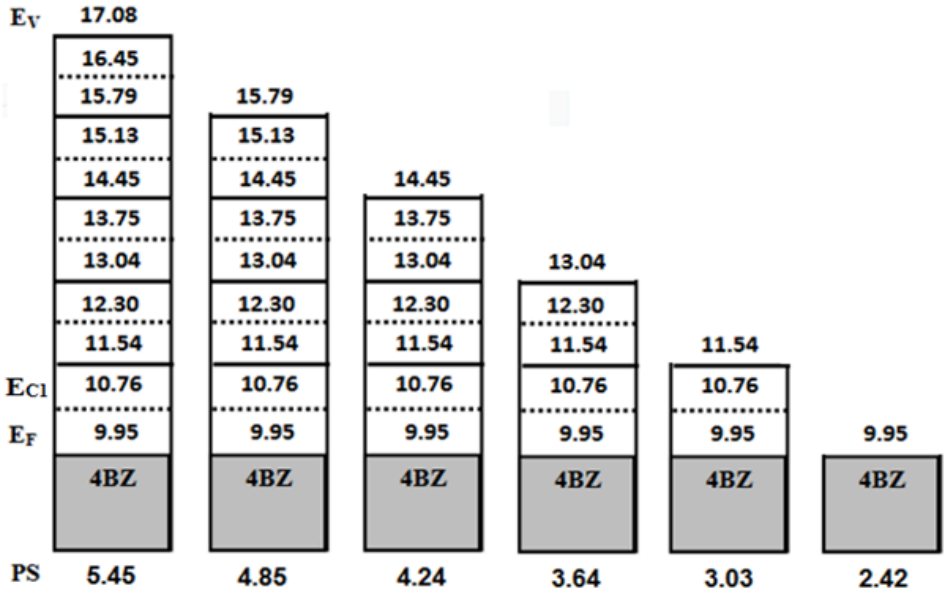

Fig. 1 Energy band structures of CdSe (Cubic) nanoparticles. Energy is in eV and PS is in nm.

Table 2 The calculated electronic parameters and transitions of Cubic CdSe.

CdSe (Cub.) V_P = 56.1 Å^3 , V_B = 4.42 Å^{-3} , PCS = 0.607 nm , SUS = 5.46 nm,

E_g = 0.81 eV, QES < 5.46 nm, RS = 2.42 nm

Particle Size (nm)	N_F	N_C	N_U	W_F eV	No. of Transitions	Possible Transitions (nm)
5.46	4	5	9	7.13	10	173.89, 190.74, +↓
4.85	4	4	8	5.84	8	212.3, 239.35, +↓
4.24	4	3	7	4.5	6	275.52, 326.27, +↓
3.64	4	2	6	3.09	4	401.24, 527.59, +↓
3.03	4	1	5	1.59	2	779.77, 1530.66

2.42	4	0	4	0	0	Escape

Fig 2 shows the energy band structures of bulk hexagonal CdSe compound and its variation with particle size. It is evident that as the particle size decreases, the BU is clipped without variation in energy gap and the energy levels are reduced. The bulk BU has $\mathbf{E_F}$ = 9.95 eV, $\mathbf{E_V}$ = 17.09 eV and the first level in the CB is $\mathbf{E_{C1}}$ =10.36 eV. The BU consists of **VB = 8BZs** and **CB = 10BZs** so that $\mathbf{N_U}$ = 18. The size of the SU of the bulk is 12.61 nm so that **QSE** <12.61 nm. It is evident that the BU of hex. CdSe is double that of cubic CdSe and so the size of **SU**. As the particle size decreases further, more clipping occurs until we get the reactive size (**RS** = 5.6 nm) at which the BU consists only of **VB** in this case $\mathbf{E_V}$ = $\mathbf{E_F}$. The detail of the band structures of hexagonal CdSe with particle size (**PS**) is given in Table 3.

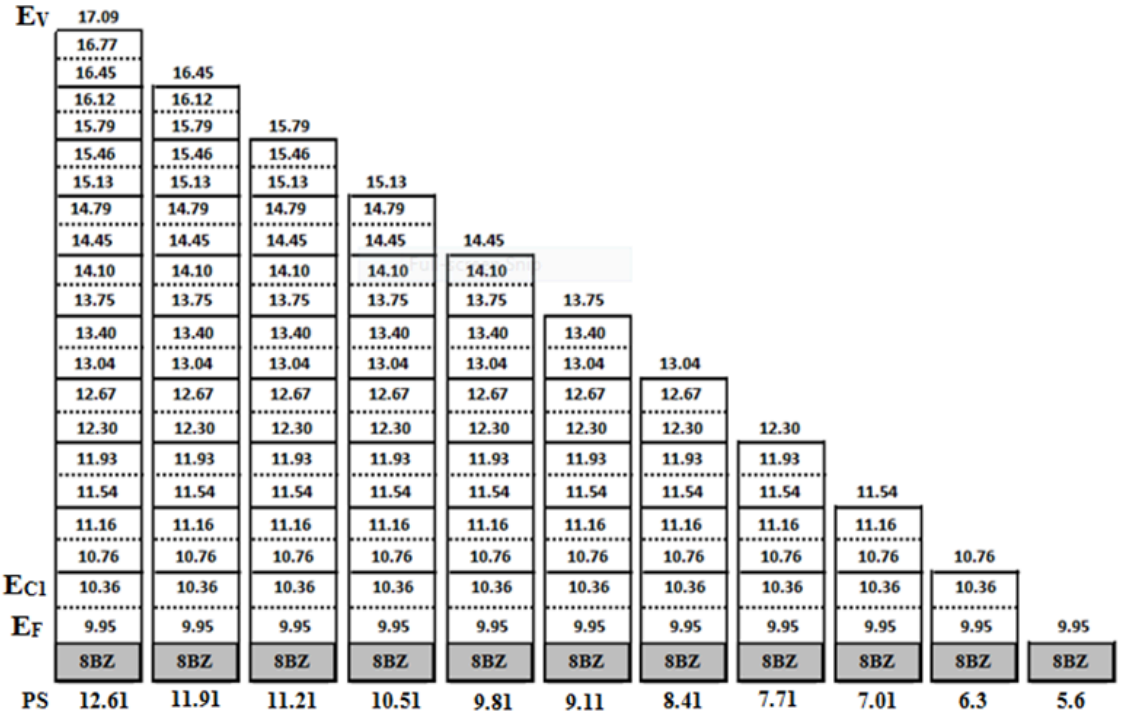

Fig. 2 Energy band structure of CdSe (Hex.) nanoparticles. Energy is in eV and PS is in nm.

Table 3: The calculated electronic parameters and transitions of Hex. CdSe.

CdSe (Hex.) V_P=112.19 Å^3 , V_B=2.21 Å^{-3} , PCS_z=0.701 nm , SUS=12.61 nm,

Eg = 0.41 eV, QES<12.61 nm, RS= 5.6 nm

Particle Size (nm)	N_F	N_C	N_U	W_F eV	No. of Transitions	Possible Transitions (nm)
12.61	8	10	18	7.14	20	173.64, 181.79, +↓
11.91	8	9	17	6.5	18	190, 200.94, +↓
11.21	8	8	16	5.84	16	212.3, 225, +↓
10.51	8	7	15	5.18	14	239.35, 256.16, +↓
9.81	8	6	14	4.5	12	275.52, 298.75, +↓
9.11	8	5	13	3.8	10	326.27, 359.37, +↓
8.41	8	4	12	3.09	8	401.24, 455.82, +↓
7.71	8	3	11	2.35	6	527.59, 626.18, +↓
7.01	8	2	10	1.59	4	779.77, 1024.66, +↓

6.3	8	1	9	0.81	2	1530.67, 3024
5.6	8	0	8	0	0	Escape

3.2 Energy gap

All crystalline materials have electronic energy band structures related to their crystal structures by Tarek's law (Eq. 1). However, the electrons in metals are free to make transitions to the conduction band while in semiconductors and insulators the electrons are not free since they are bound to the atoms. This binding energy (BE) of the electrons must be overcome first before transition. For metals BE is zero, for semiconductors BE is small and can be overcome by thermal agitation and for insulators BE is large and cannot be overcome by thermal agitation.

The energy gap ($\mathbf{E_g}$) is defined as the difference between $\mathbf{E_{C1}}$and $\mathbf{E_F}$ [23] as;

$$\mathbf{E_g = E_{C1} - E_F} \qquad (10)$$

The energy gap and the binding energy of the electron are completely different physical concepts. When a material takes an amount of energy, electrons in Fermi levels are the only electrons, which can make transition to the conduction band. This transition occurs in two steps; first, part of the absorbed energy is used to release the electron from the bonded atoms (overcome the binding energy), secondly the other part of the absorbed energy is used for the transition from VB to CB (cross the energy gap). It was found by [23] that BE for Si was found to be 0.11 eV and for diamond was 3.11 eV.

From Eq. 10 we get for cubic CdSe, $\mathbf{E_g}$ = 10.76 - 9.95= 0.81 eV and for hexagonal CdSe we get $\mathbf{E_g}$ = 10.36 - 9.95= 0.41 eV. In literature the energy gap of the bulk cubic CdSe is 1.712 [36], 1.77 [37], 2.3 eV [38] and for bulk hexagonal CdSe is 1.74 [39], 1.797 [36], 1.7 eV [38]. If we take the average $\mathbf{E_g}$ for both structures, we get for cubic $\mathbf{E_g}$ =1.927 eV and for hex. $\mathbf{E_g}$ = 1.745 eV. We can determine BE of the electron in both structures which, in this case, it is the difference between the experimental measured value and the calculated value of the energy gap. By calculation we get for cubic CdSe, BE = 1.927-0.81=1.117 eV and for hex. CdSe, BE = 1.745-0.41=1.335 eV. This means that the electrons in hex. CdSe structure are more tightly bound than in cubic structure. These values for BE indicates the semiconducting nature of CdSe in both structures.

For CdSe hexagonal nanorods with diameter 25 nm and length 82 nm the energy gap was found to be $\mathbf{E_g}$ = 1.68 eV [39]. For CdSe hexagonal nanoparticles with size varies from 13 to 18 nm, $\mathbf{E_g}$ varies from 1.68 to 1.71 eV [40]. For CdSe quantum dots (QDs) with size 5 nm, it was found to be 1.88 eV [41]. For CdSe cubic nanoparticles with size 1.45 nm, $\mathbf{E_g}$ = 3.51 eV [36]. Actually, this size (1.45 nm) for cubic CdSe QDs is smaller than the calculated reactive size, which is 2.42 nm. This means that at this size, the BU consists only of VB and in this case, there are no transitions but emission of electrons if they acquire any energy.

3.3 Work Function

The work function **WF** is defined, in CALQQM [22], as the difference in energy between the internal vacuum level $\mathbf{E_V}$ and the Fermi level $\mathbf{E_F}$ and is given by;

$$\mathbf{WF = E_V - E_F} \qquad (11)$$

The calculated **WF** for cubic CdSe bulk was found to be 7.13 eV and that of hexagonal CdSe was 7.14 eV. Fig. 3 shows the variation of **WF** with particle size for both cubic and hex. CdSe. It is clear that **WF** decreases by decreasing particle size until it reaches zero at **PS**= 2.42 nm for cubic and at **PS**= 5.6 nm for hex. CdSe. **WF** of both structures of CdSe (cubic and hexagonal) converges to -5.45 eV at zero size. The experimental measured **WF** for hexagonal bulk CdSe was found to be 6.62 eV by [42]. This value was measured by taking the onset of photoelectric yield per quanta. If the photon energy, at which half the number of electrons were emitted, was taken, **WF** will be about 7.15 eV, which match very well the calculated value (7.14 eV, see Table 2 and Table 3).

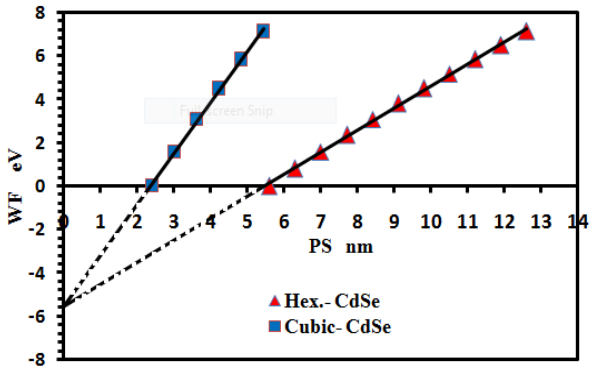

Fig. 3 The variation of the workfunction WF with particle size PS for Hex. and cubic CdSe

3.4 Possible Transitions

When a material takes an amount of energy, the electrons in $\mathbf{E_F}$ are the only electrons, which can make transitions to the higher levels. Therefore, the electronic transitions will be from $\mathbf{E_F}$ to the higher levels according to the band structure of each material and the excitation energy. As long as this amount of energy is less than **WF**, the electrons stay in the material. If the energy is more than **WF**, the electrons will leave the material. The energy given to the electrons must match the energy difference between the two levels in order to make transition. The possible electronic transitions for the two structures of CdSe are given in Table 2 and Table 3. The BU of the bulk hexagonal CdSe ($\mathbf{N_U}$ =18) is double that of the cubic CdSe ($\mathbf{N_U}$ = **9**). Therefore, the possible transitions in the hexagonal CdSe are double that in cubic CdSe. Moreover, all the possible transitions in cubic CdSe are included in hexagonal CdSe possible transitions. The possible transitions in the bulk hex. BU ranges from 173.64 (UV) to 3024 nm (IR). The possible transitions decrease by decreasing the particle size because the BU is clipped due to the clipping of SU. The smallest BU has two possible transitions 1530.67 and 3024 nm in IR region.

Let us take some experimental evidences on the calculated transitions. For CdSe hexagonal nanoparticles with size varies from 13 to 18 nm, it was found that a photoluminescence (PL) emission spectra display high intensity band edge emission peak centered at 678 nm [40]. This peak is close to the calculated value 626.18 nm. In addition, PL emission spectra showed broadband with maximum peak at 556 nm for CdSe QDs with size 5 nm [41]. Moreover, it was found by [43] that the first absorption peak and the emission peak of the synthesized CdSe cores are 516 nm and 529 nm respectively. These values are very close to the calculated value 527.56 nm. Two peaks in PL spectra was found by [44], the first peak at 560 nm and the second peak at 460 nm. Another peak was observed by [45] at 457 nm for CdSe QDs with size between 15 to 20 nm. These peaks are close to 527.59 nm and 455.82 nm calculated peaks. PL peak was observed by [37] centered at 325 nm which is very close to the calculated 326.27 nm transition. It is clear that all the observed spectra are within the predicted transitions by EPMN.

4. Conclusions

In conclusion, the energy levels of the bulk and nanostructures are discrete and can be calculated using Tarek's law. As the particle size decreases, the SU is clipped and consequently the BU is clipped. The clipping of BU reduces the energy levels and the work function **WF** of the particle without variation in energy gap. Consequently, the electronic properties of the particles will change according to the new BU. By applying Egypt pyramids model EPMN on the semiconductor compound CdSe, the quantum size effect **QSE** and the reactivity size **RS** were calculated to be 5.45, 2.42, 12.61, 5.6 nm for cubic and hexagonal CdSe respectively. The observed peaks in absorption and photoluminescence spectra, 678, 529, 457, and 325 nm match very well the calculated transitions 626.18, 527.59, 455.82, and 326.27 nm respectively.

Conflicts of Interest

There are no conflicts to declare.

Funding Statement

There is no any funding for this work.

Acknowledgments

Thanks to all contributors of publishing this work.

References

1. Brus, L. E., J Chem Phys, 79, 11, (1983).
2. Goldstein, A. N.; Echer, C. M.; Alivisatos, A. P., Science, 256, 5062, (1992).
3. Tolbert, S. H.; Alivisatos, A. P., Annu Rev Phys Chem, 46, 595-625, (1995).
4. Y. W. Cao, U. Banin, J. Am. Chem. Soc. 122**,** 9692, (2000).
5. X. G. Peng, L. Manna, W. D. Yang, J. Wickham, E. Scher, A. Kadavanich, A. P. Alivisatos, Nature, 404, 59 (2000).
6. L. Manna, E. C. Scher, A. P. Alivisatos, J. Am. Chem. Soc.Ul, 12700, (2000).
7. L. Qu, Z. A. Peng, X. Peng, Nano Letters, 1, 6, (2001).
8. T. Mokari, U. Banin, Chem. Matt., l5, 3955, (2003).
9. Quantum Dot Market; (2021).
10. Abdellatif, A. A. H.; Younis, M. A.; Alsharidah, M.; Al Rugaie, O.; Tawfeek, M. H., Int J Nanomed, 17, (2022).
11. Yekimov, A. I.; Onushchenko, A. A., JETP Lett+, 34, 6, (1981).
12. Yekimov, A. I.; Onushchenko, A. A., Sov Phys Semicond+, 16, 7, (1982).
13. Dingle, R., Advances in Solid State Physics, Queisser, H. Ed.; Vol. XV; Vieweg, (1975).
14. Efros, A. L.; Efros, A. L., Sov Phys Semicond+, 16, 7, (1982).
15. Yekimov, A. I.; Onushchenko, A. A.; Plyukhin, A. G.; Efros, A. L., Sov. Phys. JETP, 61, 4, (1985).
16. Baskoutas S, Terzis AF., J Appl Phys 99, 013708, (2006).
17. Segets D, Lucas JM, Taylor RNK, Scheele M, Zheng H, Alivisatos AP, et al, Acs Nano; 6, 9021–32, (2012).
18. Moreels I, Lambert K, Smeets D, De Muynck D, Nollet T, Martins JC, et al, Acs Nano; 3, 3023–30. (2009).
19. Sotirios Baskoutas and Andreas F. Terzis, J. Appl. Phys. 99, 013708, (2006).
20. G. Dong et al, Frontiers in Materials, 2, 1, (2015).
21. Tarek El Ashram, J. of Advances in Physics, 13, 8, (2017).
22. Tarek El Ashram, Alfarama Journal of Basic & Applied Sciences, 5, I, (2024).
23. Tarek El Ashram, Journal of Advances in Physics, 23, (2025).
24. S. K. J. Al-Ani, H.H. Mohammed, E.M.N. Al-Fwade. Renewable Energy, 25, (2002).
25. S. Kang, C.K. Kumar, Z. Lee, K. Kim, C. Huh, E. Kim. Applied Physics Letters, 93, (2008).
26. A. J. Nozik. Physica E, 14, (2002).
27. K. Rajeshwar, N.R. de Tacconi, C.R. Chenthamarakshan. Chemistry of Materials, 13, (2001).
28. F. C. Luo. Journal of Vacuum Science and Technology, 16, (1979).
29. D. K. Ghosh, P.J. Samanta. Infrared Physics, 26, (1986).
30. Lev Isaakovich Berger, Semiconductor Materials, CRC Press. p. 202, ISBN 0-8493-8912-7, (1996).
31. Ninomiya S, Adachi S, J Appl Phys, 78, 7, (1995).
32. Li K, Lu Y, Fu XL, He J, Lin X, Zheng J et al InfoMat 3, 10, (2021).
33. Luo L-B, Xie W-J, Zou Y-F, Yu Y-Q, Liang F-X, Huang Z-J, Zhou K-Y et al., Opt Express, 23, 10, (2015).
34. Ashraf Malik H, Aziz F, Asif CM, Raza E, Najeeb MA, Ahmad Z et al, J Lumin, 180, (2016).
35. International Center for Diffraction Data, "PCPDFWIN," vol. PCPDFWIN v 2.3, 19081-2389, (2002).
36. Prachi Chopade, Shweta Jagtap and Suresh Gosavi, Woodhead Publishing Series in Electronic and Optical Materials, Science Direct, P. 105-153, (2020).
37. Mahesh Verma, D. Patidar, K. B. Sharma and N. S. Saxena, Journal of Nanoelectronics and Optoelectronics, 10, (2015).
38. R. B. Kale and C. D. Lokahande, Semicond. Sci. Technol., 20, (2005).

39. G. Ramalingam, N. Melikechi, P. Dennis Christy, S. Selvakumar, and P. Sagayaraj, Journal of Crystal Growth, 311, 11, (2009).

40. Prachi Chopade, Somnath Bhopale, Shweta Jagtap, Mahendra More, and Suresh Gosavi, J. of Mat. Sc. Mat. in Elec., 35, 161, (2024).

41. Fida Muhammad, Muhammad Tahir, Muhammad Zeb, Muttanagoud N. Kalasad, Suhana Mohd Said, Mahidur R. Sarker, Mohd Faizul Mohd Sabri and Sawal Hamid Md Ali, Scientific Reports, 10, 4828, (2020).

42. Robert K. Swank, Phy. Rev., 153, 3, (1967).

43. Junjie Hao, Haochen Liu, Jun Miao, Rui Lu, Ziming Zhou, Bingxin Zhao, Bin Xie, Jiaji Cheng, Kai Wang and Marie-Helene Delville, Scientific Reports, 9, 12048, (2019).

44. Azam Sobhani and Masoud Salavati-Niasari, J. Mater. Sci: Mater Electron., 26, 6836, (2015).

45. Neupane Dipesh, Kathmandu University Journal of Science, Engineering and Technology, 8, II, (2012).